

## Normal and superconducting states of MgCNi<sub>3</sub> upon Fe and Co substitution and external pressure

T. Geetha Kumary,\* J. Janaki, Awadhesh Mani, S. Mathi Jaya, V. S. Sastry, Y. Hariharan, T. S. Radhakrishnan, and M. C. Valsakumar

*Materials Science Division, Indira Gandhi Centre for Atomic Research, Kalpakkam 603 102, India*

(Received 18 February 2002; published 15 August 2002)

Results of our study on the superconducting and normal-state properties of the recently discovered superconductor MgCNi<sub>3</sub>, the effect of Fe and Co substitution at the Ni site and the effect of pressure are reported. It is shown that a two band model provides a consistent interpretation of the temperature dependence of the normal-state resistance and the Hall constant. Whereas band structure calculations suggest an increase in  $T_c$  upon partial substitution of Ni with Fe and Co, Co substitution quenches superconductivity and Fe substitution leads to an increase followed by a decrease in  $T_c$ . The observed variation of  $T_c$  may be explained in terms of competition between an increase in  $T_c$  due to increase in density of states and a decrease due to spin fluctuations. Based on these results, it is suggested that the spin fluctuations are weaker in Fe doped samples as compared to the Co doped ones. An initial decrease in  $T_c$  (and the normal-state resistance) followed by an increase is observed on application of pressure. The decrease in  $T_c$  for small applied pressures can be understood in terms of the decrease in the density of states at the Fermi level. The subsequent increase in  $T_c$  with pressure is due to a lattice softening or a structural phase transition, consistent with the band structure calculations. It is conjectured that suppression of spin fluctuations by pressure may also be responsible for the observed increase in  $T_c$  at higher pressures.

DOI: 10.1103/PhysRevB.66.064510

PACS number(s): 74.25.Fy, 74.25.Jb, 74.62.Dh

### I. INTRODUCTION

The recent discovery<sup>1</sup> of superconductivity in the intermetallic compound MgCNi<sub>3</sub> has initiated a number of studies aimed at elucidating the nature of its normal and superconducting states. Apart from the fact that it is the first known superconducting compound which has a perovskite structure without oxygen, the interest is mainly due to the preference of superconductivity over ferromagnetism which is rather unexpected in a compound whose main ingredient is Ni. By proposing an electronic analogy with the superconducting oxide perovskites, He *et al.*<sup>1</sup> suggested that holes in the Ni  $d$  states might be responsible for electrical conduction in this compound. The signs of the measured Hall constant<sup>2</sup> and thermoelectric power<sup>3</sup> are, however, consistent with normal state transport occurring mainly due to electronlike carriers. Most of the normal-state transport properties, such as the electrical resistivity  $\rho(T)$ , Hall coefficient  $R_H(T)$  and thermoelectric power  $S(T)$ , show unusual temperature dependence. They are not amenable to a single unified description encompassing the low- and high-temperature regimes. For example, the Hall coefficient is almost temperature independent below 140 K, but, its magnitude decreases<sup>2</sup> with increase in temperature above 140 K. Even though the conventional Bloch-Grüneisen expression provides a good fit above 70K, a power law seems<sup>2</sup> to be better for  $\rho(T)$  below 70 K. An electronic crossover occurring at  $T_* \sim 50$  K was proposed<sup>3</sup> to account for these anomalies. The normal-state NMR properties of MgCNi<sub>3</sub> are also anomalous<sup>4</sup> and similar to what is seen in the exotic superconductor Sr<sub>2</sub>RuO<sub>4</sub>. Observation<sup>5</sup> of a zero bias conductance peak in the tunneling spectrum is argued to be a signature of unconventional pairing (as in the case of Sr<sub>2</sub>RuO<sub>4</sub>) in this compound. The

NMR measurement<sup>4</sup> below  $T_c$ , on the other hand, shows a coherence peak whose magnetic field dependence is consistent with  $s$ -wave pairing. The temperature dependence of the electronic specific-heat below  $T_c$  is consistent<sup>6</sup> with the conventional electron-phonon mechanism for superconductivity. Analysis<sup>1</sup> of the specific heat data suggests that this compound is a moderately strong-coupled (electron-phonon coupling constant  $\lambda \sim 0.77$ ) superconductor. The observed<sup>2</sup> temperature dependence of  $H_{c2}$  is typical of a conventional superconductor in the dirty limit. Thus a complete understanding of the superconducting and normal states of this compound is yet to emerge.

There have been a number of first principle electronic structure calculations using tight binding linear muffin tin orbital (TB-LMTO),<sup>7-9</sup> full potential linear muffin tin orbital (FP-LMTO),<sup>10</sup> and full potential linear augmented plane wave (FP-LAPW)<sup>11-13</sup> methods, within the local density approximation (LDA), to understand the electronic and magnetic properties of MgCNi<sub>3</sub> and related compounds. LDA +  $U$  calculations<sup>14</sup> on MgCNi<sub>3</sub> with  $U = 5$  eV yields essentially the same band structure as that of the LDA, indicating that electron-correlation effects of Ni- $3d$  electrons are unimportant in this compound. This is consistent with the fact that the measured value of the Wilson ratio<sup>15</sup> is only 1.15, typical of a system with modest electron-correlation effects. The results of these calculations are quite sensitive to the methods employed and also to the numerical values of the parameters. The general features of the band structure (which, however, are essentially the same in all these calculations) can be briefly summarized as follows: There is a strong hybridization between the Ni- $3d$  electrons and the C- $2p$  electrons and thus carbon plays the crucial role of the mediator of electron hopping. Two of the bands cross the Fermi level  $E_f$  and

hence both of them contribute to conduction. The density of states at the Fermi level [ $N(E_F)$ ] is predominantly due to Ni-3*d* electrons. One of the distinguishing features of the density of states of this compound is a sharp peak around 80 meV (its location is very sensitive to the method of calculation) below  $E_F$  arising from the  $\pi$  antibonding states of Ni-3*d* and C-2*p* states. The Stoner enhancement<sup>16</sup> is moderately strong to cause ferromagnetic spin fluctuations, but, not strong enough to obtain a ferromagnetic ground state.

It is well known that the perovskite structure is conducive to a variety of interesting physical phenomena such as superconductivity, magnetism, colossal magnetoresistance, etc. Soon after the announcement<sup>1</sup> of the discovery of superconductivity in MgCNi<sub>3</sub>, TB-LMTO calculations were performed<sup>7</sup> to obtain guidelines for synthesis of related compounds with interesting physical properties. The results of the calculations for the pristine MgCNi<sub>3</sub> are consistent with the reports now available in the literature.<sup>8-13</sup> Our calculations showed that MgCMn<sub>3</sub>, MgCFe<sub>3</sub>, and MgCCo<sub>3</sub> may form, but they would be magnetic. Replacement of Mg with other alkaline-earth elements Ca, Sr, and Ba would be interesting. For example, CaCNi<sub>3</sub>, CaCFe<sub>3</sub>, and SrCCo<sub>3</sub> would be magnetic, whereas SrCNi<sub>3</sub>, BaCNi<sub>3</sub>, and CaCCo<sub>3</sub> would be nonmagnetic. As mentioned earlier, band structure calculations showed that the Fermi level in MgCNi<sub>3</sub> lies towards the right side of a peak in the density of states (DOS)  $N(E)$ . Removal of half an electron per formula unit would shift the Fermi level to the peak in the DOS. Within the rigid band approximation (RBA), this can be achieved by substitution of Ni<sub>3</sub> by Ni<sub>5/2</sub>Co<sub>1/2</sub> or Ni<sub>11/4</sub>Fe<sub>1/4</sub>. Our spin-polarized supercell calculations for MgCNi<sub>3-x</sub>M<sub>x</sub> showed an increase (but much less than the RBA estimate) in  $N(E_F)$ , and more importantly, *absence* of a magnetic moment, for  $x=1/4$  and  $1/2$  ( $M=Co$ ) and  $x=1/4$  ( $M=Fe$ ). Hence an increase in  $T_c$  is expected until  $x=1/2$  for  $M=Co$  and  $x=1/4$  for  $M=Fe$ . Furthermore, our calculations suggest a structural instability when the lattice parameter is changed either way. In particular, a lattice instability is conspicuous (in the calculation) at a modest estimated pressure of  $\sim 2$  GPa. Hence effect of application of pressure in this system would also be interesting. In what follows, we present the results of our analysis<sup>17,18</sup> of the normal-state resistance, the variation in superconducting properties upon Fe and Co substitution, and the effect of pressure on the superconducting transition temperature and normal-state resistance of MgCNi<sub>3</sub>.

## II. SAMPLE PREPARATION AND CHARACTERIZATION

In addition to the pure MgCNi<sub>3</sub>, a series of compounds MgCNi<sub>3-x</sub>M<sub>x</sub> ( $x=0.05, 0.15,$  and  $0.30$  for  $M=Fe$ ;  $x=0.05, 0.10, 0.20,$  and  $0.40$  for  $M=Co$ ) were prepared in order to investigate the effect of hole doping. The samples were prepared by following the solid state reaction route described by He *et al.*<sup>1</sup> Starting materials used were Mg (99.8%), Ni (99.99%), Fe (99.999%), Co (99.99%), and amorphous carbon (99%), all in the form of powder. 20% excess of Mg is taken in the starting mixture in order to compensate for the loss of Mg due to evaporation. Also an excess of 50% C is taken to obtain the optimum carbon

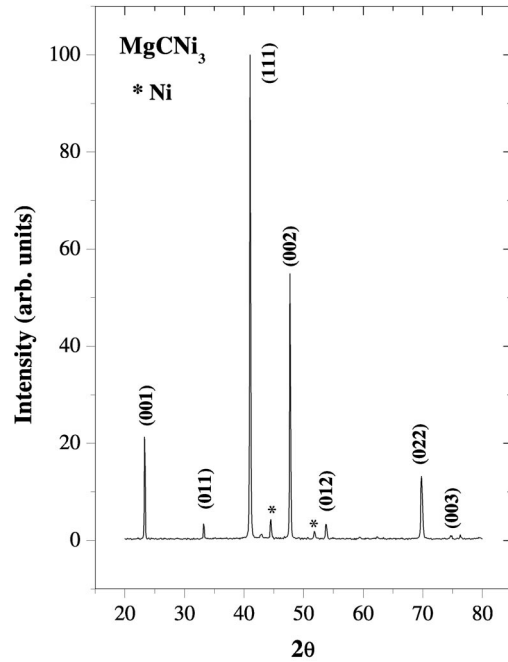


FIG. 1. X-ray diffraction pattern of pristine MgCNi<sub>3</sub>. The lines marked with an asterisk correspond to unreacted Ni.

stoichiometry<sup>1</sup> in the compound. The raw materials were mixed thoroughly and were pressed into pellets. The pellets were subjected to the heating schedule described by He *et al.*,<sup>1</sup> in an atmosphere of 92% Ar and 8% H<sub>2</sub>.

The crystal structure of all the samples are characterized by x-ray diffraction. Ac susceptibility and four-probe dc resistance have been measured in the range 4.2–300 K using home-made dipsticks. The high pressure resistance measurement has been carried out for the pristine MgCNi<sub>3</sub> using a pressure locked opposed Bridgman anvil apparatus<sup>19</sup> using the four-probe method. A superconducting Pb manometer is used for pressure calibration. We have also characterized the microstructure of MgCNi<sub>3</sub> with SEM.

## III. RESULTS AND DISCUSSION

The x-ray patterns of the undoped and doped samples are consistent with a perovskite structure with the space group  $Pm\bar{3}m$ . Small amounts of unreacted Ni (2–5%) and MgO impurity (<2%) were present in some of the samples. Except for these blemishes, all the samples are of good quality, with sharp x-ray diffraction peaks. The XRD pattern for MgCNi<sub>3</sub> is shown in Fig. 1 as an example. The lattice parameter for the unsubstituted MgCNi<sub>3</sub> was found to be 3.810 ( $\pm 0.0004$ ) Å which is in agreement with the values reported in the literature. No significant change in lattice parameter was noticed upon partial substitution of Ni with Fe or Co. This observation is consistent with the very small variation of the lattice parameter  $a(x=0)=3.806$  Å,  $a(x=3)=3.802$  Å, seen in the study of MgCNi<sub>3-x</sub>Co<sub>x</sub> by Ren *et al.*<sup>20</sup>

The variation of resistance  $R$  with temperature  $T$  of the pristine MgCNi<sub>3</sub> is shown in Fig. 2. It can be seen that the

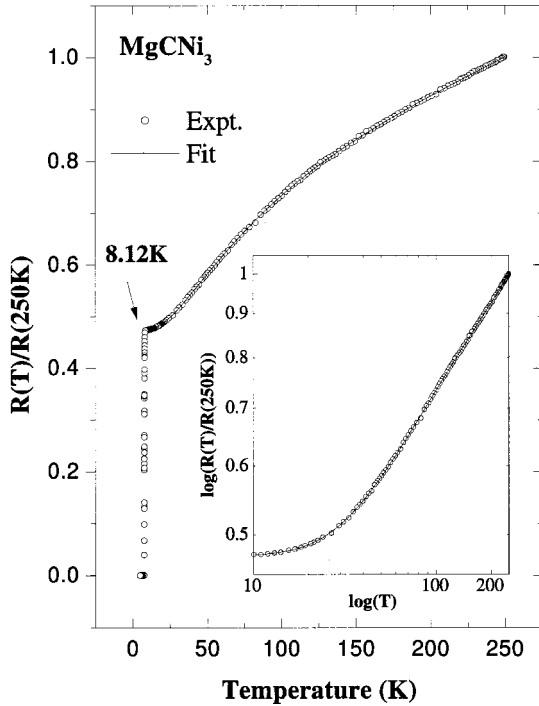


FIG. 2. Resistance as a function of temperature for pristine MgCNi<sub>3</sub>. The continuous line is a fit to a two band model of conduction. The normal state resistance is plotted as a function of temperature on a log-log scale in the inset to show that the fit is indeed very good in the entire range.

shape of the  $R(T)$  curve presented here is very similar to those reported by He *et al.*<sup>1</sup> and Li *et al.*<sup>2</sup> The residual resistivity ratio of this sample [ $R(300\text{ K})/R(10\text{ K})$ ] is 2.2 similar to that obtained by He *et al.*<sup>1</sup> However, the magnitude of the resistivity obtained in this study is approximately 30 times more than that of He *et al.*<sup>1</sup> and 10 times that of Li *et al.*<sup>2</sup> This discrepancy can be understood in terms of the possible differences in the microstructure that can be expected from the fact that unlike in the study of He *et al.*,<sup>1</sup> our samples were not subjected to high pressure sintering. Figure 3 shows an SEM pattern of one of the MgCNi<sub>3</sub> samples. The fractal character of the sample, which is quite evident from

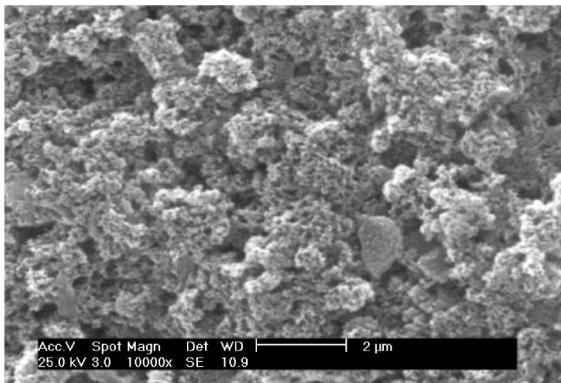


FIG. 3. Microstructure of a MgCNi<sub>3</sub> sample. Fractal-like character of the sample can be seen.

this photograph, entails a much longer and corrugated path (as compared to the bulk) for the electrons. This makes the usual procedure of multiplying the resistance by the (external) area/length of the sample to get the resistivity  $\rho$  erroneous.<sup>21</sup> Since the actual path length of the electrons in such a poorly connected medium is longer than that in the bulk, the apparent resistance will be larger than what is expected from a scaling based merely on the external geometry.<sup>21</sup> Hence there is a need for a geometric renormalization while converting resistance into resistivity in sintered samples. Our sample is more loosely packed (compared to that of He *et al.*<sup>1</sup>) and hence the larger apparent resistivity of our sample. A superconducting transition with an onset (mid)  $T_c$  of 8.13 K (7.69 K) is observed (90–10% of the transition width  $\Delta T_c = 0.34\text{ K}$ ). The ac susceptibility measurement (see Fig. 7) shows a lower  $T_c$  (onset  $T_c = 7.35\text{ K}$ ) consistent with the values reported in literature.<sup>1</sup>

#### A. Analysis of normal state resistance

Assuming compliance with Matheissen's rule, we have tried to fit the normal-state resistance of MgCNi<sub>3</sub> with the expression for a conventional metal

$$R(T) = A + BT^2 + CG(T, \Theta). \quad (1)$$

In Eq. (1), the constant  $A$  represents the contribution to resistance from electron-impurity scattering,  $BT^2$  term accounts for the contribution to resistance from electron-electron scattering and also from spin fluctuations, and the last term represents the electron-phonon scattering. In order to get some insight into the nature of the (transport) electron-phonon coupling function  $\alpha_{\text{tr}}^2 F(\omega)$ , the fitting was performed with two possible functional forms for  $G(T, \Theta)$ : (1) the Bloch-Gruneisen function

$$G(T, \Theta) = \left(\frac{1}{z}\right)^n \int_0^z dx \frac{x^n}{[(e^x - 1)(1 - e^{-x})]}, \quad z = \frac{\Theta}{T},$$

$$n = 3 \text{ or } 5,$$

that takes into account the scattering of the electrons with all the (acoustic) phonons, and (2) the Einstein form

$$G(T, \Theta) = \frac{z}{(e^z - 1)(1 - e^{-z})}, \quad z = \frac{\Theta}{T}$$

which allows for coupling of the electrons with a specific phonon mode. We found that the Einstein model gave a better fit to the resistivity data of MgCNi<sub>3</sub> at ambient and high pressures than the Bloch-Gruneisen model. This clearly shows that the electron-phonon coupling function  $\alpha_{\text{tr}}^2 F(\omega)$  in MgCNi<sub>3</sub> is sharply peaked at the frequency  $\omega_*$  given by  $\hbar\omega_* = k_B\Theta$ , where  $k_B$  is the Boltzmann constant.

The coefficient  $B$  obtained using the fit turns out to be negative and also the fitted value of the Debye temperature ( $\Theta \sim 110\text{ K}$ ) is too low. If we substitute this value of  $\Theta$  and the reported value of the electron phonon coupling constant ( $\lambda = 0.77$ ) in the McMillan's formula for  $T_c$  given by

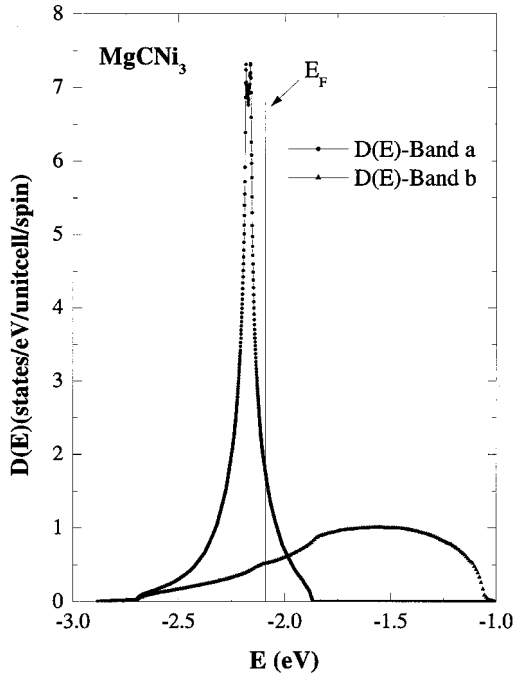


FIG. 4. Density of states corresponding to the two bands that cross the Fermi level. One band is nearly empty and the other is almost full.

$$T_c = \left( \frac{\Theta_D}{1.45} \right) \exp \left( \frac{-1.04(1+\lambda)}{\lambda - \mu^*(1+0.62\lambda)} \right), \quad (2)$$

we get the superconducting transition temperature  $T_c \sim 4$  K, much less than the experimental value (we have taken  $\mu^*$  to be 0.1).

This and the reported<sup>2</sup> temperature variation of the Hall constant are consistent with a two band model of conduction involving “light” electrons coupled to low-frequency phonons and “heavy” holes coupled to high-frequency phonons.<sup>7</sup> As mentioned in the Introduction, band structure calculations<sup>22</sup> show that two bands cross the Fermi level (see Fig. 4) one almost full (designated as band a) and the other nearly empty (band b). There are equal number of electronlike and holelike charge carriers<sup>23</sup> in this compound and the effective mass of the holelike carrier is almost ten times that of the electronlike carrier. Therefore the normal-state electrical conduction will be mainly due to electrons and hence we can expect the Hall constant to be negative. However, both the electrons and holes will be contributing to the conductivity  $\sigma(T)$  and hence  $\sigma(T)$  will be the sum of the conductivities  $\sigma_e(T)$  and  $\sigma_h(T)$  due to the electrons and holes, respectively. Therefore the effective resistivity  $\rho(T)$  can be written as

$$\rho(T) = A_0 + \frac{\rho_e(T)\rho_h(T)}{\rho_e(T) + \rho_h(T)}, \quad (3)$$

where  $\rho_e(T) = 1/\sigma_e(T)$  and  $\rho_h(T) = 1/\sigma_h(T)$ , and  $A_0$  is a constant added to take care of the effect of defects in the sample. In Eq. (3)  $\rho_e(T)$  and  $\rho_h(T)$  have separate temperature dependences

$$\rho_{e,h} = A_{e,h} + B_{e,h}T^2 + C_{e,h}G(T, \Theta_{e,h}). \quad (4)$$

With  $B_e$  and  $B_h$  both positive, it is possible to obtain an effective resistivity such that a fit with Eq. (1) would give a negative  $B$ .

The continuous line in Fig. 2 is a fit<sup>24</sup> of the normal-state resistance  $R(T)$  using the two band model for conduction given by Eq. (3). It can be seen from the figure that the fit is very good—the root mean square fractional deviation

$$\sqrt{\frac{1}{N} \sum_{i=1}^N \left( \frac{\rho^{\text{expt}}(T_i) - \rho^{\text{fit}}(T_i)}{\rho^{\text{expt}}(T_i)} \right)^2}$$

between the observed ( $\rho^{\text{expt}}$ ) and fitted ( $\rho^{\text{fit}}$ ) values of the resistivities, is found to be less than 0.0015.  $\Theta_e$  ( $\sim 110$  K) obtained from the fit is seen to be smaller than  $\Theta_h$  ( $\sim 250$  K). That is, the electronlike carriers are coupled to low-frequency phonons as compared to holelike carriers which are coupled to higher frequency phonons. Assuming the value of the hole-phonon coupling constant  $\lambda$  to be the same as that obtained from the specific heat measurement,<sup>1</sup> we get a  $T_c$  comparable to the experimental value. Thus we can infer that superconductivity in MgCNi<sub>3</sub> is due to holelike carriers. Since  $\rho_e(T)$  is much less than  $\rho_h(T)$ , the effective resistivity  $\rho(T)$  will be close to  $\rho_e(T)$  and hence the value of  $\Theta$  that one gets with a fit of  $\rho(T)$  to Eq. (1) will be close to  $\Theta_e$ .

Assuming phonons associated with rotation and breathing of CNi<sub>6</sub> octahedra to be important for superconductivity in MgCNi<sub>3</sub>, Singh and Mazin<sup>11</sup> performed a frozen-phonon zone-corner calculation of the electron-phonon interaction parameter  $\lambda$ . Their calculations showed that the octahedral rotation mode (with the estimated frequency  $\sim 105$  cm<sup>-1</sup> = 151 K) has a larger coupling with the charge carriers than the breathing mode (with the estimated frequency  $\sim 349$  cm<sup>-1</sup> = 502 K). Detailed investigations are necessary to see if the charge carriers that couple to the octahedral rotation modes are holelike or not. It is also worth investigating the effect of anharmonicity on the mode frequency and  $\lambda$ . The question is will the frequency of the octahedral rotation mode get renormalized from 151 to  $\sim 250$  K which is inferred to be important for superconductivity on the basis of the analysis of resistivity?

The reported variation of the Hall constant  $R_H(T)$  can also be qualitatively explained in the two band model. The Hall constant  $R_H(T)$  is the weighted sum of the Hall constants  $R_{He}$  and  $R_{Hh}$  due to the electrons and holes, respectively, and it is given by

$$R_H = \frac{(R_{He}\sigma_e^2 + R_{Hh}\sigma_h^2)}{(\sigma_e + \sigma_h)^2} = R_{He} \left[ \frac{1 - \left( \frac{\rho_e}{\rho_h} \right)}{1 + \left( \frac{\rho_e}{\rho_h} \right)} \right]. \quad (5)$$

Since the number of electrons is equal to the number of holes  $R_{Hh} = -R_{He}$  and hence  $R_H < 0$ . If  $d/dT(\rho_e/\rho_h) > 0$ , then the magnitude of  $R_H$  also will decrease with temperature thus explaining the reported Hall effect behavior. We thus see that a consistent interpretation of the temperature dependence of

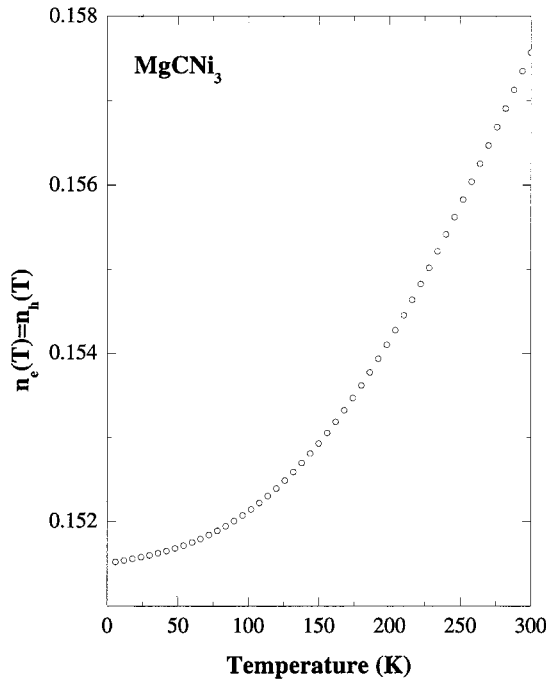


FIG. 5. Temperature dependence of the concentration  $n_e(T)$  and  $n_h(T)$  of electronlike and holelike carriers (Ref. 23), respectively. Both of these increase by  $\sim 4\%$  when temperature increases from 0 to 300 K.

both the normal state resistivity and the Hall constant can be achieved by invoking a two band model of conduction. It remains to be seen whether the same physical picture can provide a satisfactory interpretation of the anomalies seen in the thermopower and NMR relaxation rate.

We have also tried to study the effect of the proximity of the peak in the density of states (van Hove singularity) close to the Fermi level on the resistivity. It is seen<sup>7</sup> that the chemical potential *increases* with temperature. As a result of this, some of the electrons from the almost filled band go to the almost empty band [the number of electrons  $n_b(T)$  in the almost empty band increases at the expense of the number of electrons  $n_a(T)$  in the almost full band<sup>23</sup>]. Thus the numbers of both electronlike and holelike carriers increase with temperature. As can be seen from Fig. 5, carrier concentration increases by approximately 4% when the temperature is raised from 0 to 300 K. This is one of the reasons why the resistivity is not linear in temperature even in the high-temperature regime.

**B. Effect of Fe and Co substitution**

Figures. 6 and 7 represent the superconducting transitions traced by the resistance and susceptibility measurements respectively for the Co substituted compounds. The transition temperature decreases monotonically with increase in Co concentration, similar to the results now available in the literature.<sup>20,25</sup> The variation of the midpoint  $T_c$  with respect to  $x$ , the Co concentration, is shown as an inset of Fig. 6. The decrease in the diamagnetic signal (and hence the superconducting volume fraction) can also be seen in Fig. 7, which

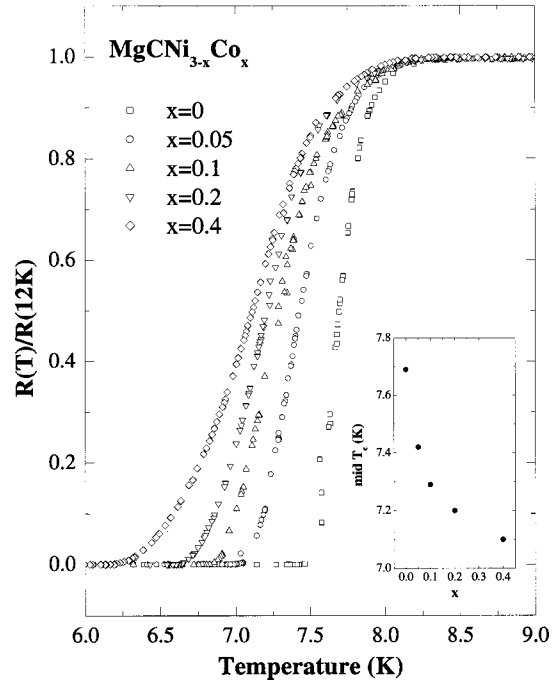


FIG. 6.  $R$  vs  $T$  for the Co substituted samples for various concentrations  $x$  of Co.  $T_c$  decreases and the transition width  $\Delta T_c$  increases monotonically with  $x$ .  $T_c$  corresponding to the midpoint of the resistive transition is shown in the inset.

again is consistent with the results reported in the literature.<sup>25</sup> Fe substitution, on the other hand, leads to an increase in  $T_c$  followed by a decrease. The superconducting transitions traced for the Fe substituted compounds are shown in Figs. 8

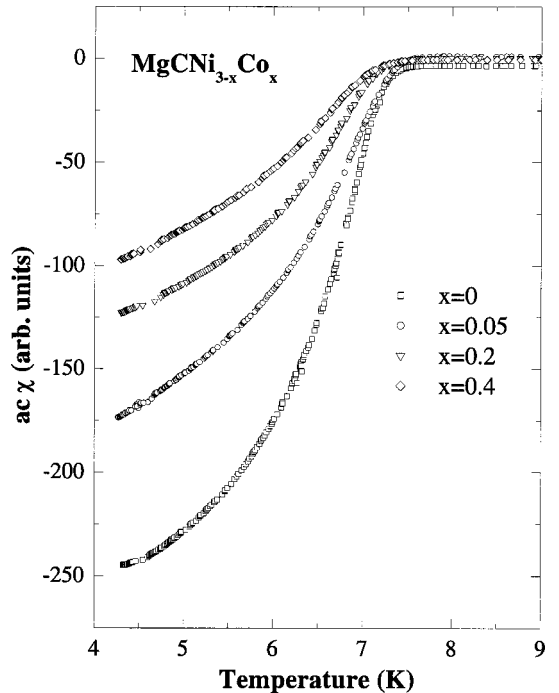


FIG. 7.  $ac \chi$  vs  $T$  for the Co substituted samples for various concentrations  $x$  of Co.  $T_c$  as well as the diamagnetic signal (hence the superconducting volume fraction) decreases with  $x$ .

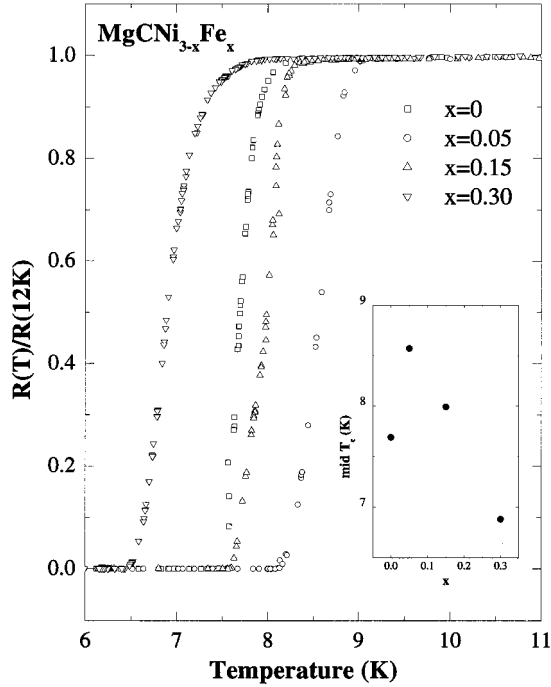


FIG. 8.  $R$  vs  $T$  for the Fe substituted samples for various concentrations  $x$  of Fe.  $T_c$  corresponding to the midpoint of the superconducting transition is shown in the inset. Notice the nonmonotonic behavior of  $T_c$ .

and 9. The maximum  $T_c$  is obtained when the Fe concentration is 0.05. The onset of the superconducting transition occurs at 9 K for this sample in our resistivity scan. Increasing Fe concentration beyond 0.05 is found to suppress  $T_c$ . The inset of Fig. 8 represents the midpoint  $T_c$  as a function of Fe concentration.

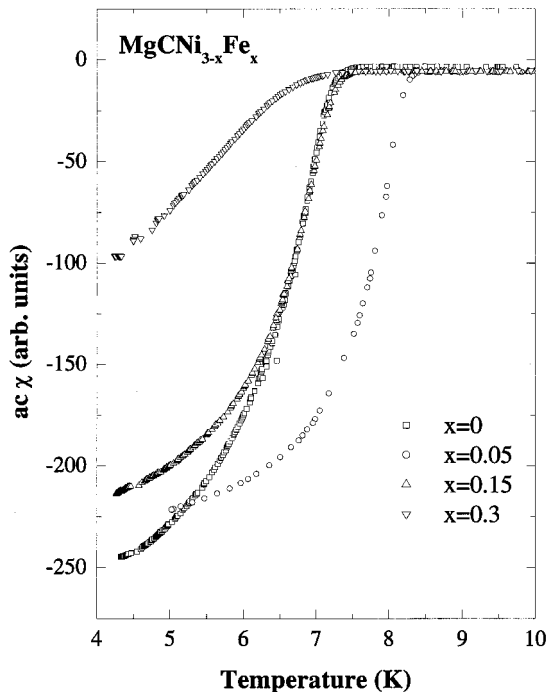


FIG. 9.  $ac \chi$  vs  $T$  for the Fe substituted samples.

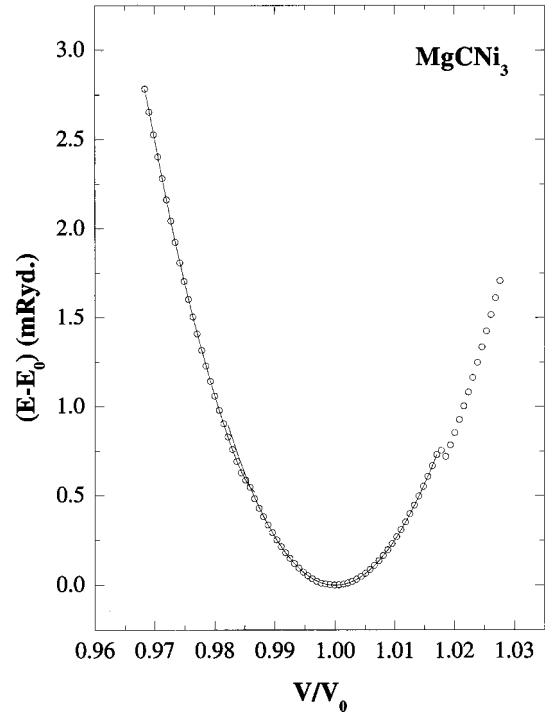


FIG. 10. Total energy of  $\text{MgCNi}_3$  as a function of  $V/V_0$ , where  $V_0$  is the equilibrium volume, obtained from band structure calculations. Notice the abrupt change of slope near  $V/V_0 \sim 0.985$  as well as the nonmonotonic behaviour near  $V/V_0 \sim 1.02$ .

An increase in  $T_c$  was expected for Fe substitution until  $x=0.25$  and for Co substitution till  $x=0.5$ , on the basis of a simple minded interpretation of the results of the band structure calculations. However, we observed a monotonic decrease in  $T_c$  for Co substitution and an increase followed by a decrease for Fe substitution. These results are clearly at variance with what is expected from the band structure calculations. The observed variation in  $T_c$  can be explained in terms of an increase in  $T_c$  due to increase in the density of states and a decrease due to spin fluctuations: As mentioned in the Introduction, NMR measurements<sup>4</sup> have shown existence of ferromagnetic spin fluctuations in  $\text{MgCNi}_3$ . Also, magnetic susceptibility measurements have demonstrated that Co doping enhances spin fluctuations in  $\text{MgCNi}_3$ .<sup>25</sup> If we assume the pairing in  $\text{MgCNi}_3$  is of  $s$ -wave type, then it will be suppressed by coupling of electrons (more precisely, the holes) with spin fluctuations. Since we get an increase in  $T_c$  for small concentrations of Fe, we believe that the spin fluctuation effect will be relatively less for Fe substituted compounds as compared to that of Co substituted ones. This is to be verified experimentally.

### C. Effect of pressure

Figure 10 shows the variation of the total energy as a function of  $V/V_0$  ( $V_0$  is the equilibrium volume) obtained from our band structure calculations.<sup>7,22</sup> Our calculations suggest *two* lattice instabilities in the range  $[0.9684, 1.0277]$  of  $V/V_0$  that has been explored in the present study. The first is a clear change in slope at  $V/V_0 \sim 0.985$  and the other is a

blip at  $V/V_0 \sim 1.018$ . In order to gain some insight into the nature of these instabilities, we looked at the variation of  $E_F$  (the Fermi energy),  $N(E_F)$  (the DOS at the Fermi level), and the position of the Fermi level vis-a-vis the peak in the DOS with  $V/V_0$ . Both  $E_F$  and  $N(E_F)$  varied almost linearly with  $V/V_0$ . However,  $E_F$  decreased significantly (by  $\sim 25\%$ ), whereas  $N(E_F)$  showed a marginal increase (by  $\sim 5\%$ ) when  $V/V_0$  increased from 0.9684 to 1.0277. The Fermi level remained to the right of the peak in DOS for the entire range of  $V/V_0$  (that we have explored). That is,  $E_F$  did not pass through the peak in DOS. In order to see if the increase in Stoner enhancement factor [that follows from the increase in  $N(E_F)$ ] drives a magnetic instability, we performed spin-polarized total energy calculations. These calculations unambiguously established that  $\text{MgCNi}_3$  is nonmagnetic in the cubic perovskite structure when  $0.9684 \leq V/V_0 \leq 1.0277$ . Identification of the ground state structure of  $\text{MgCNi}_3$  at various pressures is an open problem worth pursuing.

Of the two instabilities mentioned above, the one at  $V/V_0 \sim 0.985$  occurs at a positive pressure and hence amenable to high pressure studies. The calculated (using TB-LMTO) bulk moduli of  $\text{MgCNi}_3$  and fcc Ni are 210 and 250 GPa, respectively. The measured bulk modulus of fcc Ni, on the other hand, is 180 GPa. Thus the LDA calculation overestimates the bulk modulus. We correct for this discrepancy by scaling the calculated bulk modulus by a factor 180/250 (the ratio of the measured and calculated bulk moduli of fcc Ni) and thus estimate the bulk modulus of  $\text{MgCNi}_3$  to be 151 GPa. With this value of the bulk modulus, we expect the lattice instability to occur at a pressure  $\sim 2$  GPa. It is known that there is no structural or magnetic phase transitions in  $\text{MgCNi}_3$  as the temperature is varied, at ambient pressure.<sup>26</sup> But, there is no investigation of the structure of  $\text{MgCNi}_3$  at high pressure. It would be of interest to do high pressure x-ray diffraction on  $\text{MgCNi}_3$  to see if the predicted lattice instability indeed occurs or not. Here we report the results of resistivity measurement up to a pressure  $\sim 7$  GPa.

The superconducting transitions and the temperature dependence of resistivity of  $\text{MgCNi}_3$  traced for different external pressures are shown in Fig. 11.  $T_c$  is found to decrease with increasing pressure up to  $\sim 1.7$  GPa and it *increases* beyond this pressure. Figure 12(a) depicts the variation of the onset  $T_c$  with respect to the applied pressure. The normal-state resistance also shows a similar trend as can be inferred from Fig. 12(b), where the variation of the resistance at 10 K is plotted as a function of the applied pressure. Thus the variation of  $T_c$  with pressure is consistent with the behavior expected of a superconductor with the conventional electron- (hole) phonon mechanism—the larger the normal-state resistivity, the higher the  $T_c$ . Band structure calculations show a monotonic decrease in  $N(E_F)$  with pressure. This would imply a monotonic decrease in the electron-phonon coupling constant  $\lambda$ , if there is no phonon softening. The fit of the resistance to Eq. (1) showed an increase in  $\Theta$  with pressure upto 2 GPa and a decrease thereafter. This implies a lattice softening commencing at 2 GPa. If we assume the usual scaling [ $\lambda \sim N(E_F)/\Theta^2$ ] of the electron- (hole) phonon coupling constant with the density of states

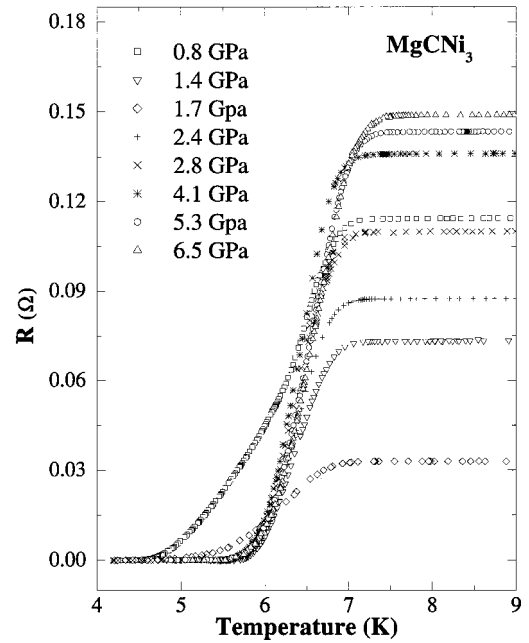


FIG. 11.  $R$  vs  $T$  of pure  $\text{MgCNi}_3$  for various pressures. The normal state resistance decreases until a critical pressure  $\sim 2$  GPa and increases thereafter.

and the Debye temperature  $\Theta$ , and calculate  $T_c$  using McMillan's formula, we find a variation of  $T_c$  with pressure that qualitatively matches with the experimental observation. It is not yet clear whether the decrease in  $\Theta$  with pressure beyond 2 GPa is due to a softening of a particular phonon mode or

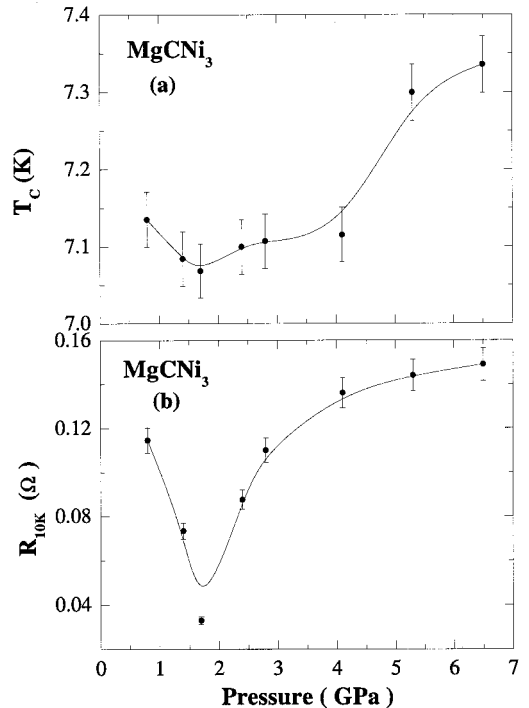


FIG. 12. (a)  $T_c$  as a function of pressure, (b)  $R_{10\text{K}}$  as a function of pressure. The continuous lines are guides to the eye. Notice the correlation between  $T_c$  and  $R_{10\text{K}}$ .

due to a structural phase transition. Another mechanism that contributes to the increase in  $T_c$  would be the suppression of spin fluctuations by pressure, thereby enhancing pairing.

Before concluding, we would like to touch upon the role of carbon, in relation to superconductivity, in this compound. It is known<sup>27</sup> that this compound can form with variable  $C$  stoichiometry. However, superconductivity is absent<sup>1,27</sup> when the  $C$  content is less than  $\sim 0.9$ . We have performed band structure calculation (using TB-LMTO) of  $\text{MgC}_{0.875}\text{Ni}_3$  by constructing an appropriate supercell.<sup>7</sup> The density of states at the Fermi level thus calculated is almost the same as that of  $\text{MgCNi}_3$ . Furthermore,  $\text{MgC}_{0.875}\text{Ni}_3$  is nonmagnetic as per this spin-polarized calculation. Thus the absence of superconductivity in  $\text{MgCNi}_3$  below a  $C$  concentration  $\sim 0.9$  is also surprising. We have, however, found a factor of 2 reduction in the height of the peak in DOS close to the Fermi level. This would support the proposal<sup>13</sup> of a possible connection between the van Hove singularity and superconductivity in  $\text{MgCNi}_3$ .

#### IV. CONCLUSIONS

To conclude, we have synthesized  $\text{MgCNi}_3$  and analyzed its superconducting and normal-state properties. We have also studied the effect of hole doping at the Ni site and the effect of application of pressure on  $\text{MgCNi}_3$ . It is found that a two band model for conduction provides a framework for

consistently explaining the observed temperature dependence of the normal-state resistance and the Hall constant. Co substitution quenches superconductivity, whereas Fe substitution causes an increase in  $T_c$  followed by a decrease. This may be understood in terms of a competition between increase in  $T_c$  due to increase in the density of states at the Fermi level and a decrease due to spin fluctuations. We speculate that spin fluctuations in Fe substituted samples are weaker than in the Co substituted samples. In fact, it is known<sup>25</sup> that there is an enhancement of spin fluctuations by Co substitution in  $\text{MgCNi}_3$ . The observed nonmonotonic variation of  $T_c$  with pressure may also be pointing out the importance of spin fluctuations vis-a-vis superconductivity in  $\text{MgCNi}_3$ . The decrease in  $T_c$  for small applied pressures can be understood in terms of the decrease in the density of states at the Fermi level. The subsequent increase in  $T_c$  with pressure is suggestive of a lattice softening or a structural phase transition, consistent with the total energy calculations. More experimental and theoretical efforts are needed to understand these issues better.

#### ACKNOWLEDGMENTS

The authors acknowledge Mrs. M. Radhika, Materials Development Division, IGCAR for providing the SEM micrographs of the  $\text{MgCNi}_3$  samples.

\*Email address: geetha@igcar.ernet.in

<sup>1</sup>T. He, Q. Huang, A.P. Ramirez, Y. Wang, K.A. Regan, N. Rogado, M.A. Hayward, M.K. Haas, J.S. Slusky, K. Inumaru, H.W. Zandbergen, N.P. Ong, and R.J. Cava, *Nature (London)* **411**, 54 (2001).

<sup>2</sup>S.Y. Li, R. Fan, X.H. Chen, C.H. Wang, W.Q. Mo, K.Q. Ruan, Y.M. Xiong, X.G. Luo, H.T. Zhang, L. Li, Z. Sun, and L.Z. Cao, *Phys. Rev. B* **64**, 132505 (2001).

<sup>3</sup>S.Y. Li, W.Q. Mo, M. Yu, W.H. Zheng, C.H. Wang, Y.M. Xiong, R. Fan, H.S. Yang, B.M. Wu, L.Z. Cao, and X.H. Chen, *Phys. Rev. B* **65**, 064534 (2002).

<sup>4</sup>P.M. Singer, T. Imai, T. He, M.A. Hayward, and R.J. Cava, *Phys. Rev. Lett.* **87**, 257601 (2001).

<sup>5</sup>Z.Q. Mao, M.M. Rosario, K. Nelson, K. Wu, I.G. Deac, P. Schiffer, Y. Liu, T. He, K.A. Regan, and R.J. Cava, *cond-mat/0105280* (unpublished).

<sup>6</sup>J.-Y. Lin, P.L. Ho, H.L. Huang, P.H. Lin, Y.-L. Zhang, R.-C. Yu, C.-Q. Jin, and H.D. Yang, *cond-mat/0202034*(unpublished).

<sup>7</sup>M. C. Valsakumar and S. Mathi Jaya, (unpublished).

<sup>8</sup>S.B. Dugdale and T. Jarlborg, *Phys. Rev. B* **64**, 100508(R) (2001).

<sup>9</sup>J.H. Shim, S.K. Kwon, and B.I. Min, *Phys. Rev. B* **64**, 180510(R) (2001).

<sup>10</sup>I.R. Shein, N.I. Medvedeva, and A.L. Ivanovskii, *cond-mat/0107010* (unpublished).

<sup>11</sup>D.J. Singh and I.I. Mazin, *Phys. Rev. B* **64**, 140507(R) (2001).

<sup>12</sup>I.G. Kim, J.I. Lee, and A.J. Freeman, *Phys. Rev. B* **65**, 064525 (2002).

<sup>13</sup>H. Rosner, R. Weht, M.D. Johannes, W.E. Pickett, and E. Tosatti, *Phys. Rev. Lett.* **88**, 027001 (2002).

<sup>14</sup>Ref. 10 cited in Ref. 9.

<sup>15</sup>Wilson ratio  $W = (\chi/\gamma)_{\text{expt}}/(\chi/\gamma)_{\text{band}}$  is defined as the ratio of the values of  $(\chi/\gamma)$  obtained from experiment and band theory.  $\chi$  is the susceptibility and  $\gamma$  is the coefficient of the linear part of the electronic specific heat.  $W=1$  for the uncorrelated case and 2 for the strongly correlated case.

<sup>16</sup>Stoner enhancement  $S = 1/(1 - \bar{S})$ , with  $\bar{S} = I_{\text{ex}}N(E_F)$ , where  $I_{\text{ex}}$  is the exchange correlation energy. The system will have a ferromagnetic instability whenever  $\bar{S} > 1$ .

<sup>17</sup>T. Geetha Kumary, J. Janaki, S. Mathi Jaya, V.S. Sastry, Y. Hariharan, T.S. Radhakrishnan, and M.C. Valsakumar, *Solid State Phys.* (to be published).

<sup>18</sup>Awadhesh Mani, T. Geetha Kumary, M.C. Valsakumar, J. Janaki, S. Mathi Jaya, V.S. Sastry, Y. Hariharan, and T.S. Radhakrishnan, *Solid State Phys.* (to be published).

<sup>19</sup>Awadhesh Mani, A. Bharathi, V.S. Sastry, Y. Hariharan, and T.S. Radhakrishnan, in *Proceedings of the Eighteenth International Cryogenic Engineering Conference (ICEC18)*, edited by K.G. Narayankhedkar (Narosa Publishing House, New Delhi, 2001), p. 615.

<sup>20</sup>Z.A. Ren, G.C. Che, S.L. Jia, H. Chen, Y.M. Ni, and Z.X. Zhao, *cond-mat/0105366* (unpublished).

<sup>21</sup>S.B. Arnason, S.P. Herschfield, and A.F. Hebard, *Phys. Rev. Lett.* **81**, 3936 (1998).

<sup>22</sup>The total energy calculations were done using the well known LMTO47 Stuttgart code that employs the tight binding linear muffin-tin orbital method within the atomic sphere approximation. von Barth-Hedin model was chosen for the exchange-correlation potential. A  $32 \times 32 \times 32$   $k$  mesh (969  $k$  points in the  $1/48$ th irreducible wedge of the Brillouin zone) was found to be adequate for the total energy to converge within 40  $\mu\text{Ry}$ .



<sup>23</sup>Band a in Fig. 4 is nearly full and band b is almost empty. Therefore the number of holelike carriers  $n_h(T) = 1 - n_a(T)$  and the number of electronlike carriers  $n_e(T) = n_b(T)$ , where  $n_a(T)$  and  $n_b(T)$  are occupancies (per spin) of band a and band b, respectively. By virtue of the relation  $n_a(T) + n_b(T) = 1$ , we find  $n_h(T) = n_e(T)$ .

<sup>24</sup>We have fitted the ratio  $R(T)/R(250 \text{ K})$  so as to eliminate the geometric renormalization factor that relates the apparent resis-

tivity to the true resistivity.

<sup>25</sup>M.A. Hayward, M.K. Haas, A.P. Ramirez, T. He, K.A. Regan, N. Rogado, K. Inumaru, and R.J. Cava, *Solid State Commun.* **119**, 491 (2001).

<sup>26</sup>Q. Huang, T. He, K.A. Regan, N. Rogado, M. Hayward, M.K. Haas, K. Inumaru, and R.J. Cava, *Physica C* **363**, 215 (2001).

<sup>27</sup>T.G. Amos, Q. Huang, J.W. Lynn, T. He, and R.J. Cava, *Solid State Commun.* **121**, 73 (2002).